



Progress in R&D on silicon edgeless strip detectors with Current Terminating Structure

**E. Verbitskaya¹, A. Cavallini², V. Eremin¹, S. Golubkov³
G. Pellegrini⁴, G. Ruggiero⁵, T. Tuuva⁶**

¹Ioffe Physico-Technical Institute RAS, St. Petersburg, Russia

²University of Bologna, Bologna, Italy

³Research Institute of Material Science and Technology

⁴Centro Nacional de Microelectrónica, CNM-IMB, Barcelona, Spain

⁵CERN, Switzerland

⁶Lappeenranta University of Technology, Finland

**13 RD50 Workshop
CERN, Geneva, Nov 10-12, 2008**

Outline

- ◆ **Overview of the approaches for rad-hard edgeless detectors**
- ◆ **Edgeless detector with CTS: design**
- ◆ **Models for potential and electric field distribution in p-on-n edgeless detector and experimental results**
- ◆ **Simulation of irradiated detectors**
- ◆ **Experimental results on CCE (test beam)**
- ◆ **Development of n-on-p edgeless detectors**

Conclusions

Requirements

Requirement: diminished dead area adjacent to detector sensitive area →

**Close-to-beam applications (CERN, TOTEM, Roman pot)
- maximal dead area width less than 50 μm**

Other applications: imaging tileable arrays for diagnostics (medicine, biology etc.)

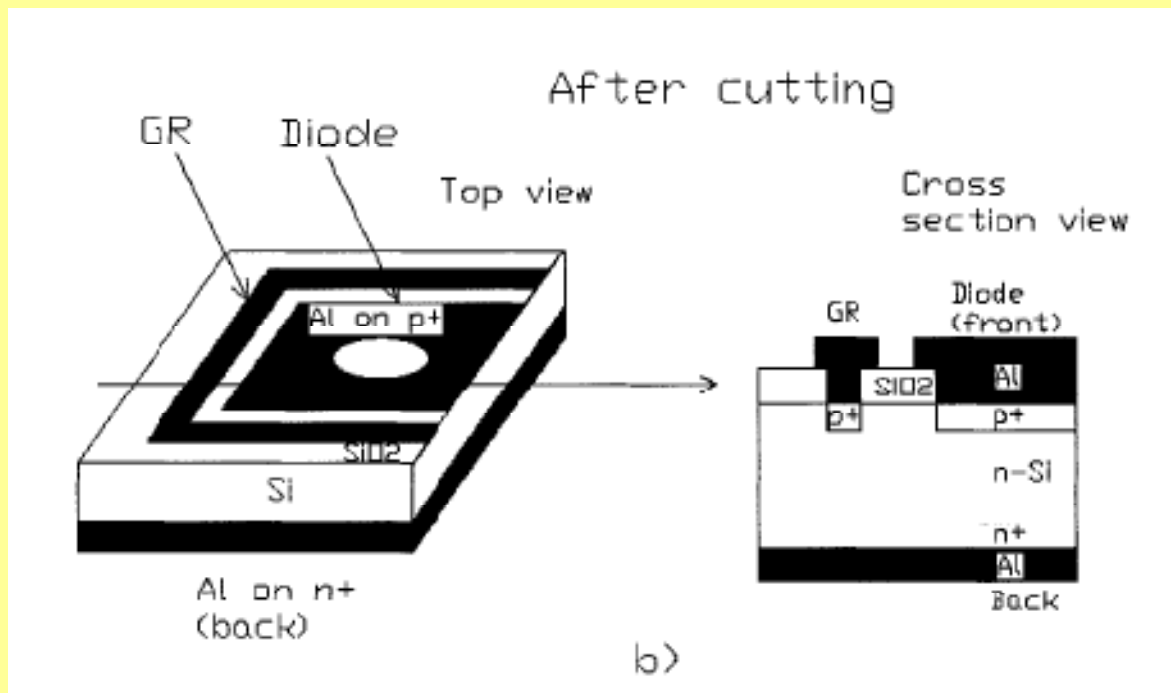
Solution: edgeless detectors (diced or cut)

Problem: elimination of the influence of high current from damaged cut on the properties of detector sensitive bulk

Prehistory

Z. Li et al., IEEE Trans. Nucl. Sci. NS-49 (2002) 1040-1046

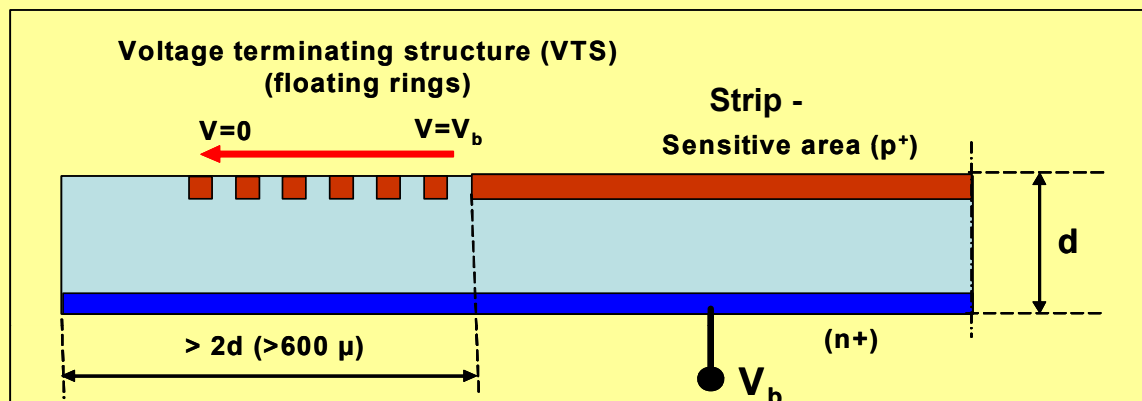
Pad detectors diced across p-n junction



I-V improvement:

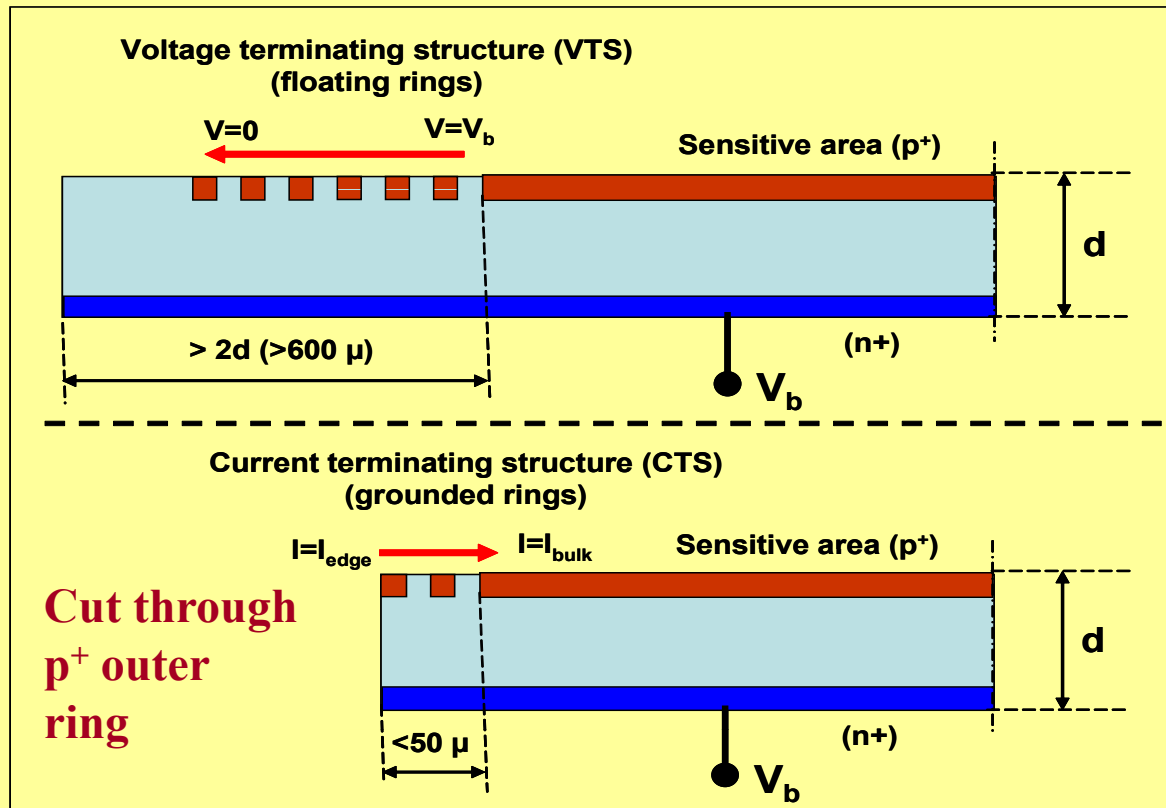
- Dicing from the back side
- Aging at RT

Overview of the approaches for edgeless detectors



Regular planar strip detector
with Voltage Terminating
Structure (VTS)

Approach: Edgeless strip detector with Current Terminating Structure (CTS)



← Regular p⁺-n-n⁺ strip detector with Voltage Terminating Structure (VTS)

← **TOTEM:**
Edgeless p⁺-n-n⁺ strip detector with CTS

1. G. Ruggiero et al. IEEE Trans. Nucl. Sci. 52 (2005) 1899.
2. E. Noschis et al. Nucl. Instr. and Meth. A 563 (2006) 41.

Alternative approach: full 3D active edge detectors

C. Da Via et al., NIM A587 (2008) 243-249

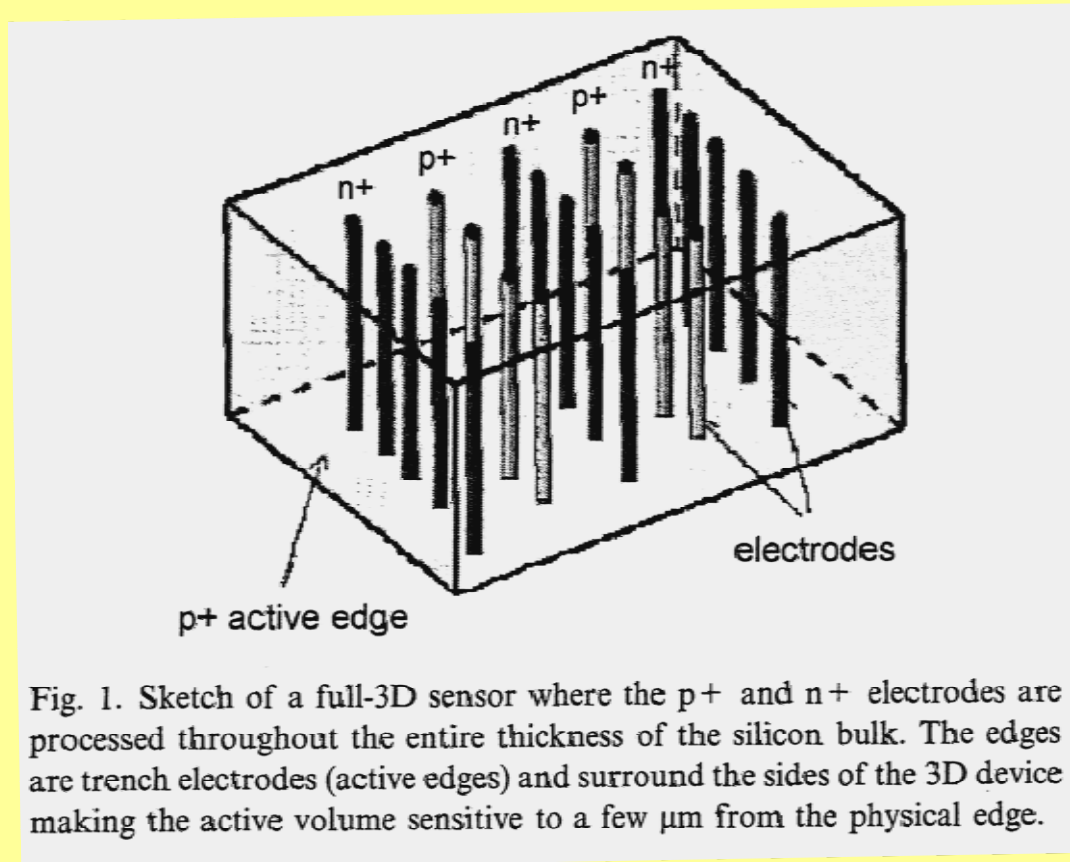


Fig. 1. Sketch of a full-3D sensor where the p+ and n+ electrodes are processed throughout the entire thickness of the silicon bulk. The edges are trench electrodes (active edges) and surround the sides of the 3D device making the active volume sensitive to a few μm from the physical edge.

Main features of design:

- p⁺ and n⁺ through entire bulk
- p⁺ active edge

- ✓ collection distance $\leq 50 \mu\text{m}$
- ✓ fast response
- ✓ higher electric field due to cylindrical geometry
- ✓ radiation hardness

but

- ✓ **Complicated technology**

*Further development of edgeless detectors with CTS:
INTAS-CERN project TOSTER:
TOtem STRip Edgeless Radiation hard detectors*

05-103-7533 Started: July 2006

CONSORTIUM

CERN - Switzerland

Ioffe Physico-Technical Institute RAS - Russia

Research Institute of Material Science and Technology - Russia

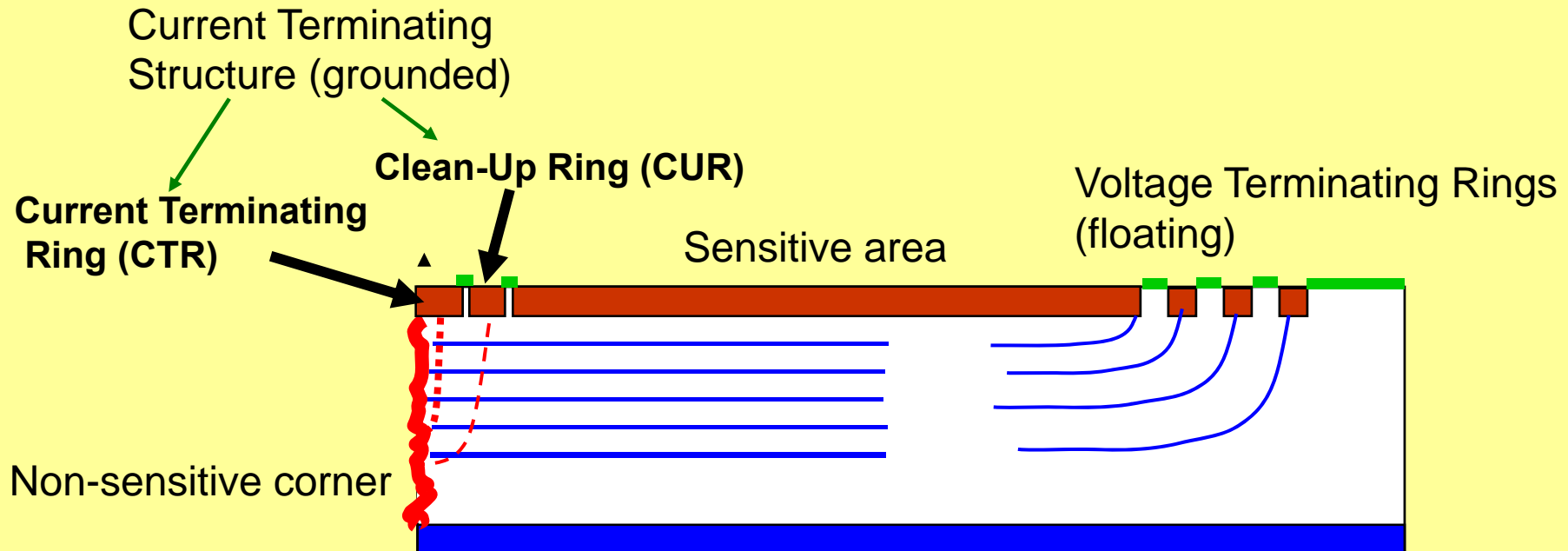
Centro Nacional de Microelectronica - CSIC – Barcelona, Spain

University of Bologna - Italy

Lappeenranta University of Technology – Finland

Head of the project: Gennaro Ruggiero (CERN)

Conceptual design of edgeless detector with CTS

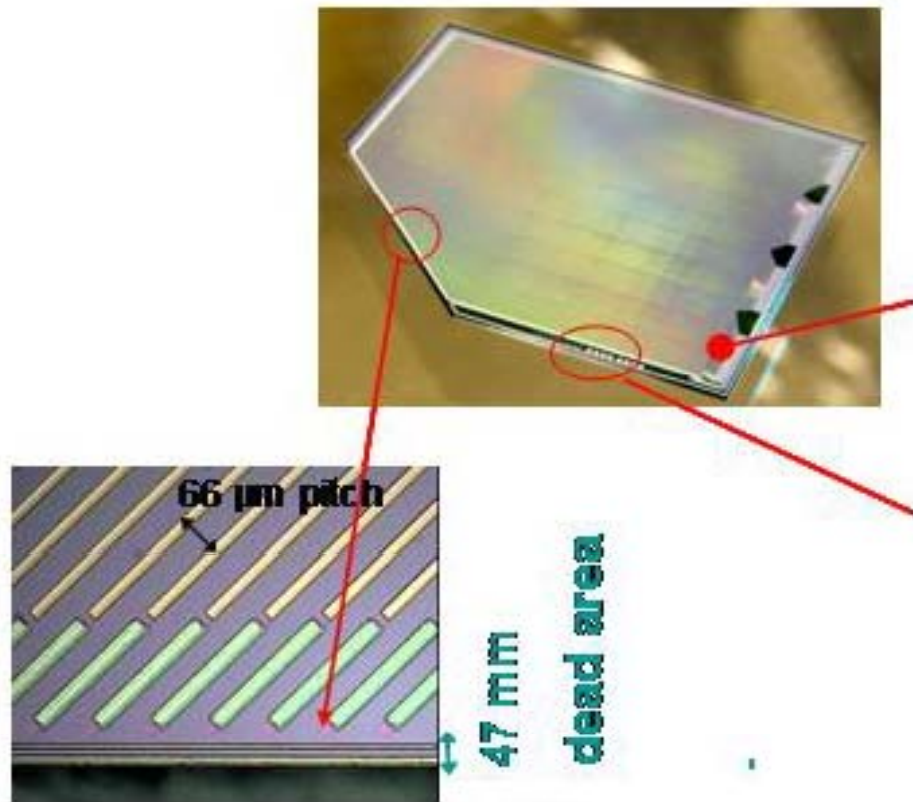


The current of CTR: ohmic current along the damaged cut

The current of CUR: diffusion current from the cut to the bulk

The current of sensitive area: bulk generated current

Performance of edgeless detector with CTS



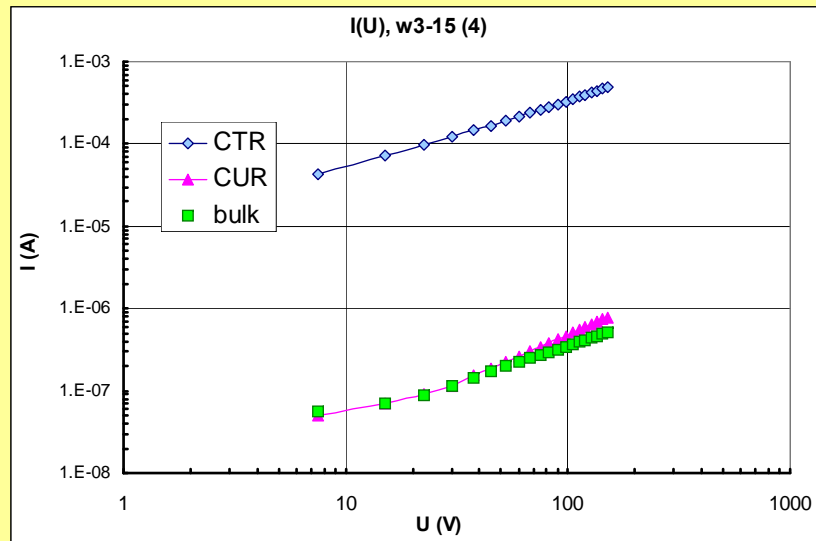
**planar technology with CTS
(Current Terminating Structure)**

Dead area 47 μm

Electrical characteristics of p-on-n edgeless detectors

Processed by Ioffe&RIMST

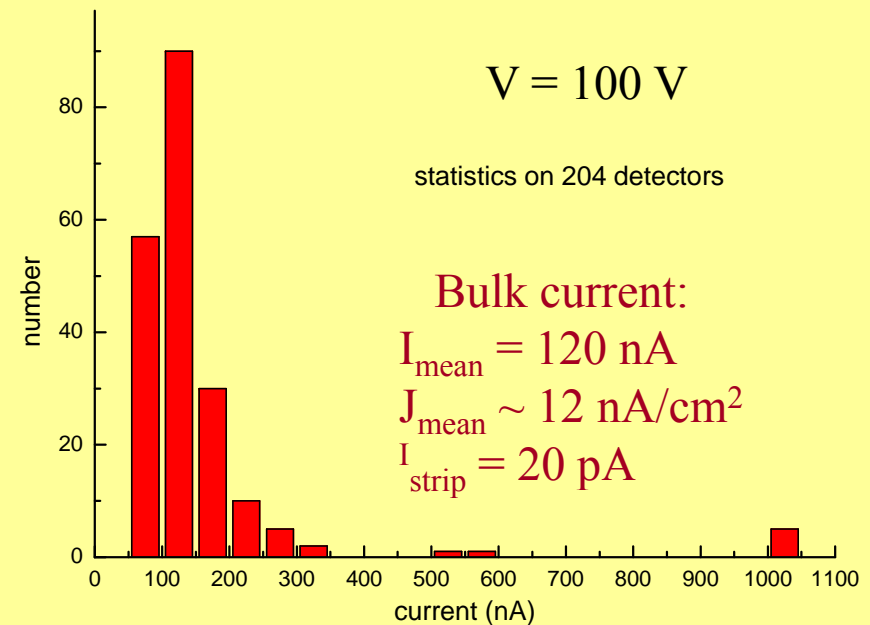
I-V characteristics



Statistics of reverse current

n-Si, $\rho \sim 20 \text{ k}\Omega\cdot\text{cm}$ $V_{fd}: \sim 20 \text{ V}$; $S = 8 \text{ cm}^2$

512 strips with a pitch of $66 \mu\text{m}$

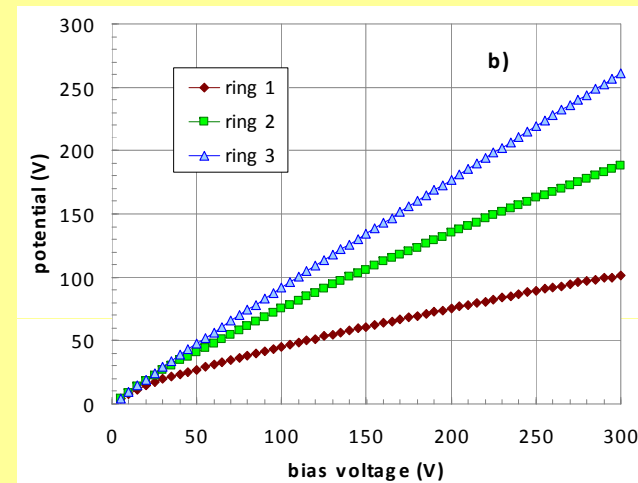
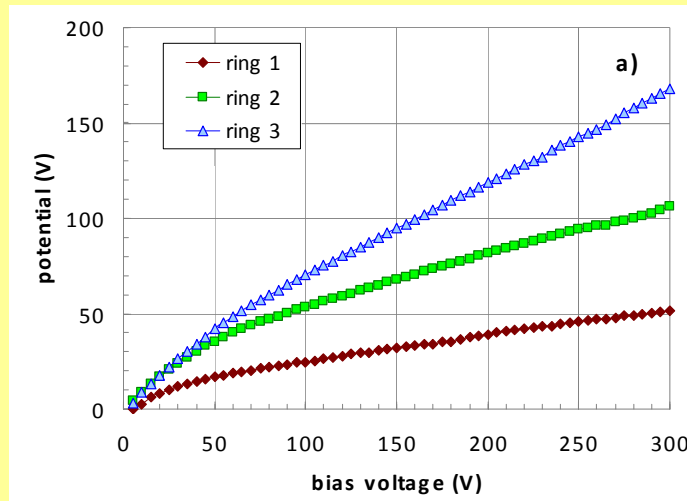


Potential distribution on VTS rings in p-on-n detector before and after scribing

Before cut

Test detectors

After cut



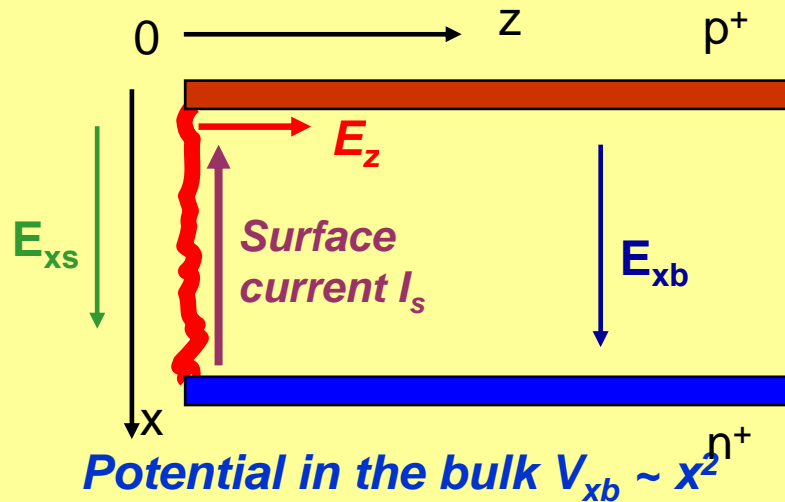
Before the cut: potential distribution occurs via punch-through effect, and potentials between the rings are distributed linearly.

After cut: potential distribution is controlled by the increased current across the damage surface (\sim mA).

VTS operates and distributes potential outside the detector active area and eventually prevents the electric field focusing at the border of the detector active area.

Models of potential and electric field distribution at the sensitive cut

Components of potential and electric field



In x direction:

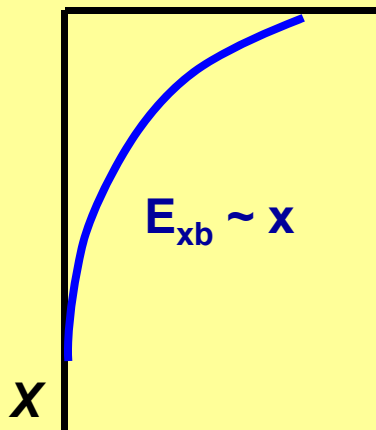
$$\left. \begin{array}{l} V_{xs}, E_{xs} \\ V_{xb}, E_{xb} \end{array} \right\} \begin{array}{l} \text{at the cut (s)} \\ \text{and inside the bulk (b)} \end{array}$$

In z direction:

E_z – normal to the cut

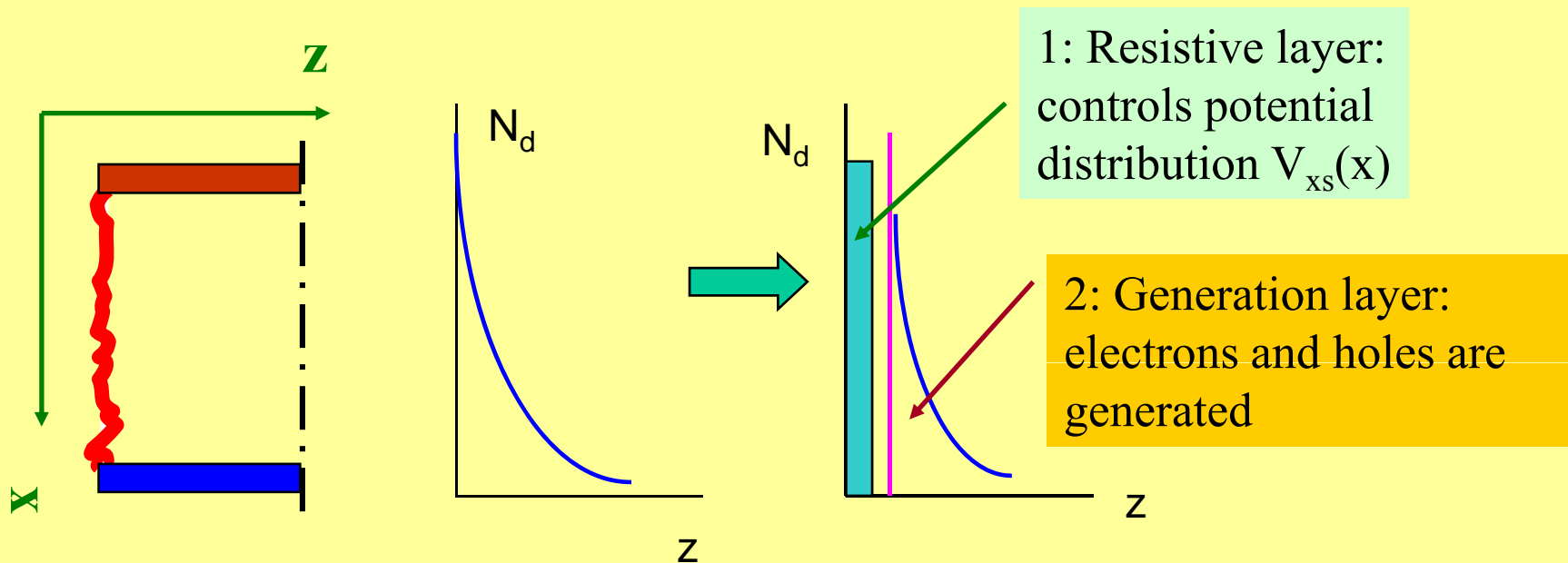
$$E_z \approx (V_{\text{surf}} - V_{\text{bulk}}) / W_z$$

W_z – distance at which V_{xs} dissipates to V_{xb}



1. Model of resistive edge layer

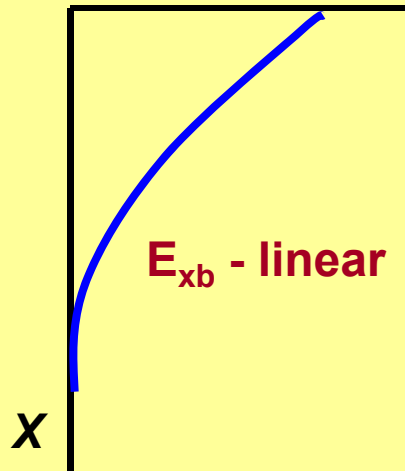
Damaged edge with high concentration of defect levels



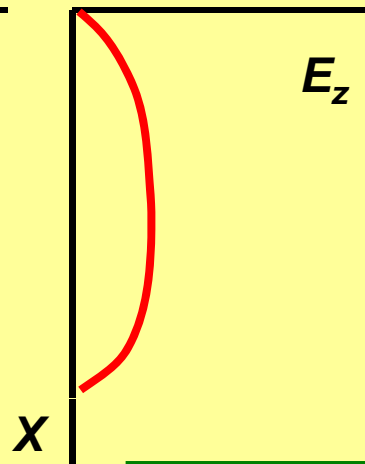
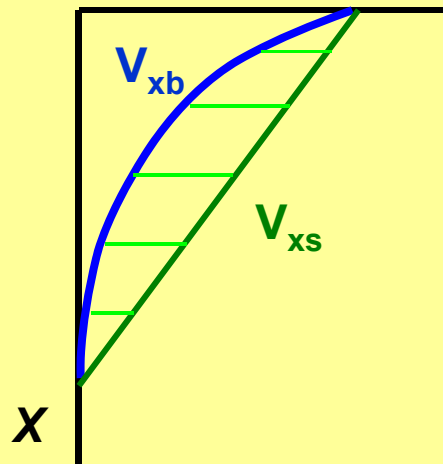
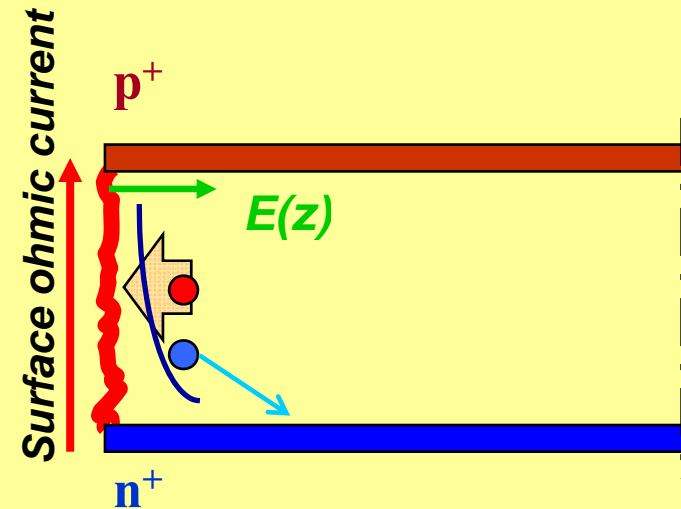
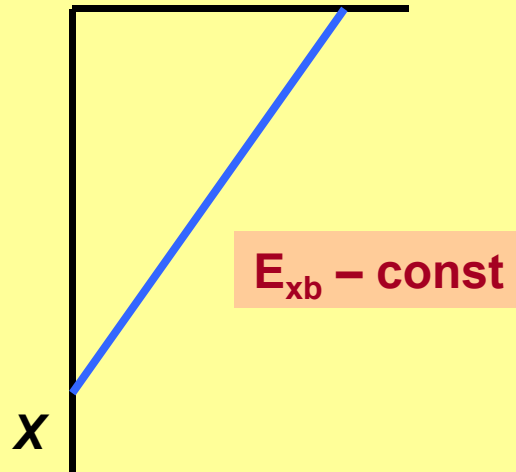
Free carriers in the generation layer do not disturb I_s and V_{xs}

Model of resistive edge layer

Potential in the bulk V_{xb}

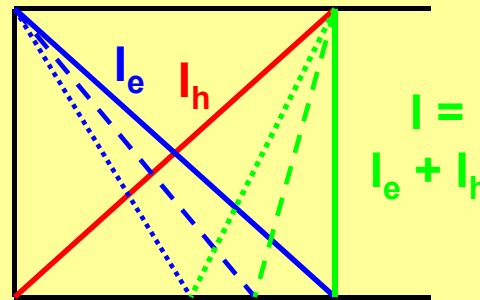
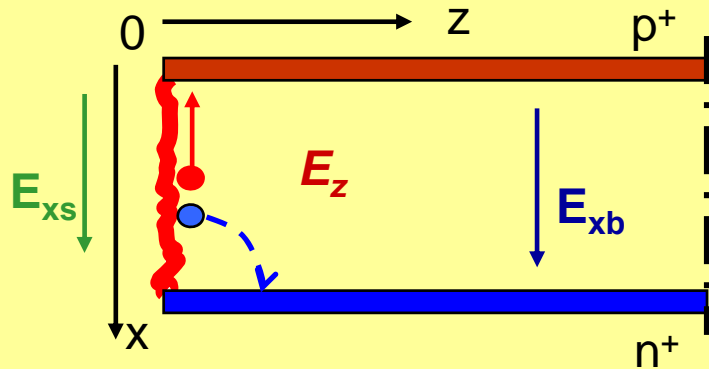


Potential at the cut V_{xs}



Generated carriers:
 holes move to CTS;
 electrons may partially flow
 inside the bulk

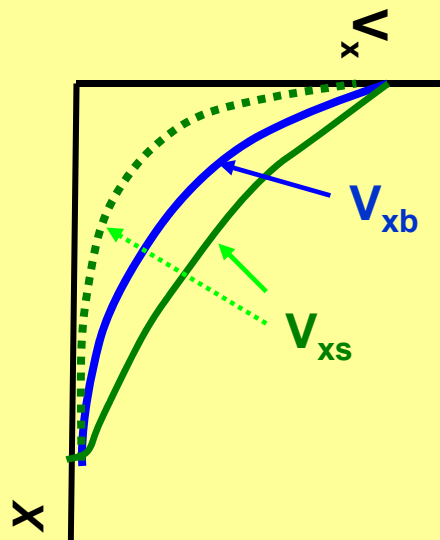
2. Model of amorphous edge layer



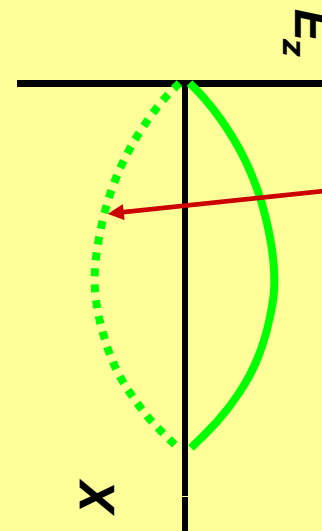
$$j_h = g_h(d - x)$$

$$j_e = (g_e - \eta_e)x$$

g – generation rate



$\eta_e \uparrow$



Inversion of E_z sign!
– forces holes to move towards the bulk

Tools for study of potential and electric field distribution

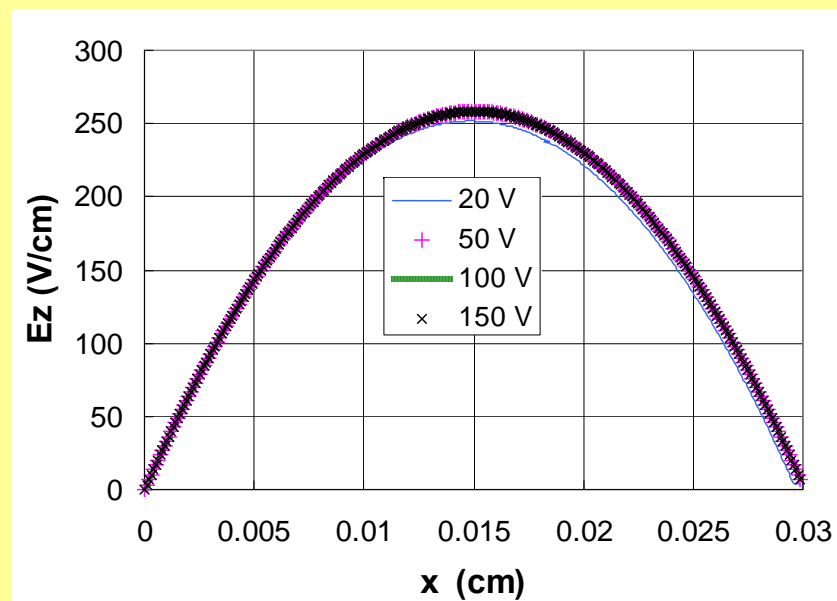
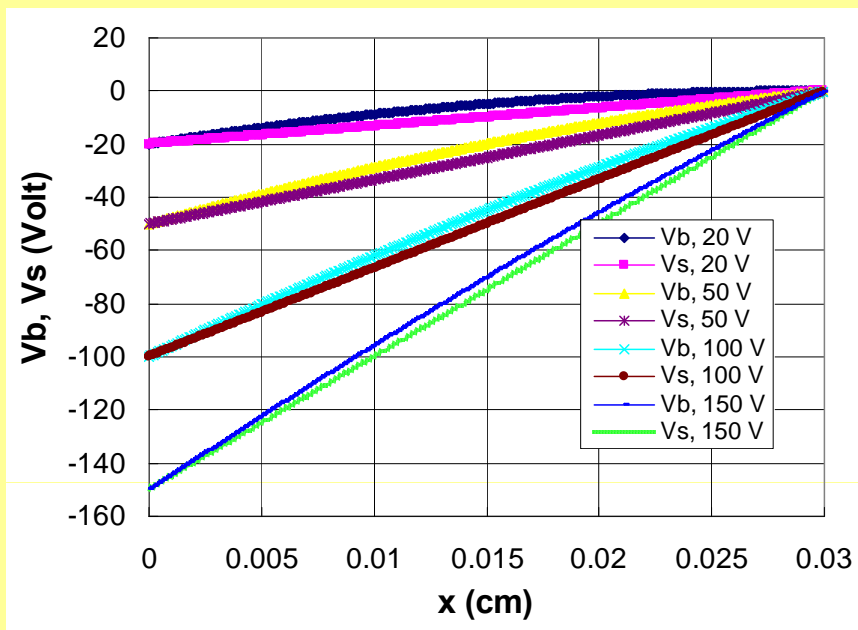
- ✓ Simulation of potential, electric field and hole trajectories (Ioffe Institute)
- ✓ Conductive MicroProbe Technique (Bologna University)
- ✓ Scanning Transient Current Technique (Ioffe Institute)
- ✓ E(x) simulation using ISE-TCAD with implemented Poisson and continuity equations (CNM Barcelona)

Additionally:

- ✓ Optical Beam Induced Current (Bologna Univ.)
- ✓ Scanning Electron Microscope (LUT)

Simulations: potential and electric field distribution, resistive edge

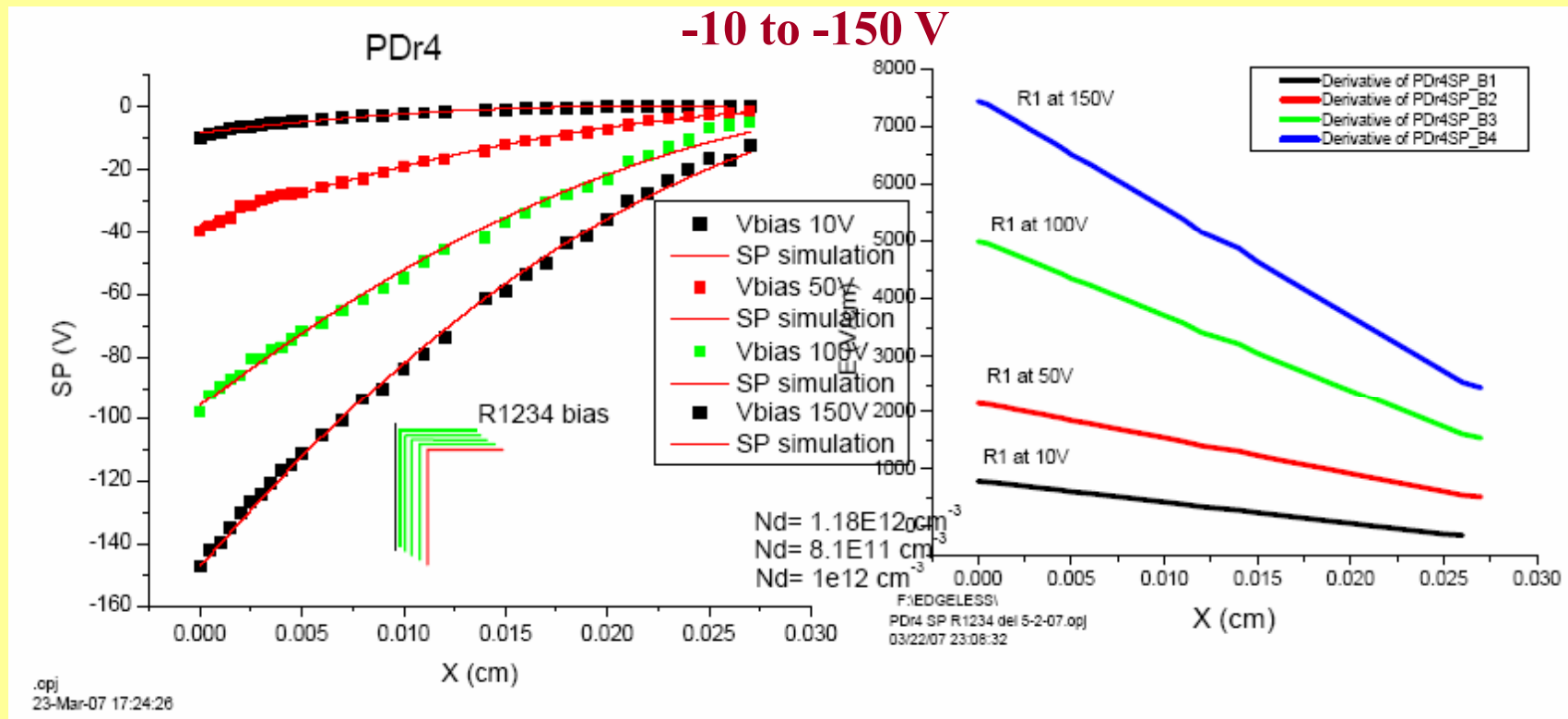
$$N_{\text{eff}} = 3 \cdot 10^{11} \text{ cm}^{-3}; V_{fd} = 15 \text{ V}$$



$$E_z \approx (V_{\text{surf}} - V_{\text{bulk}}) / W_z$$

$$W_z = 300 \text{ } \mu\text{m}$$

Experimental results on MicroProbe Technique: surface potential $SP(x)$, and $E(x)$ at the cut edge



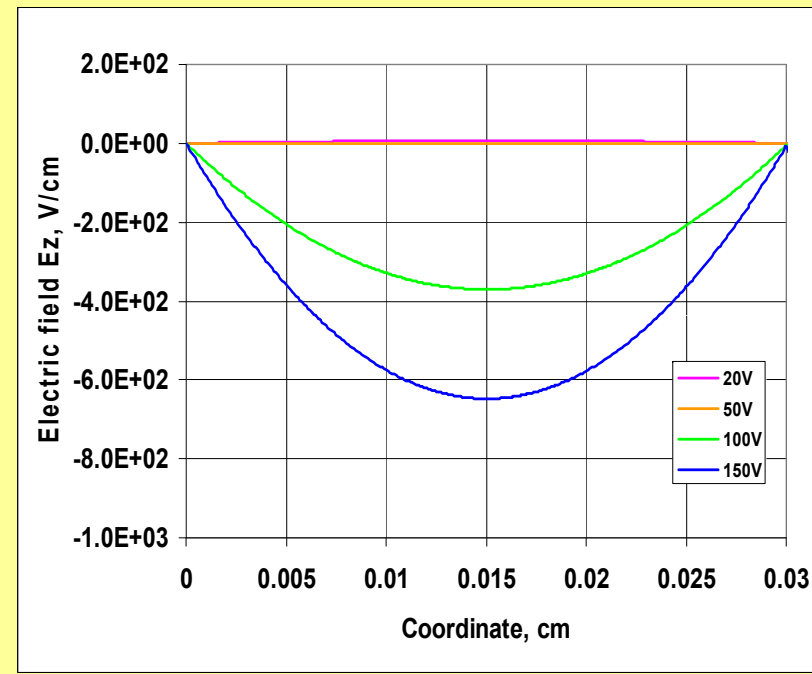
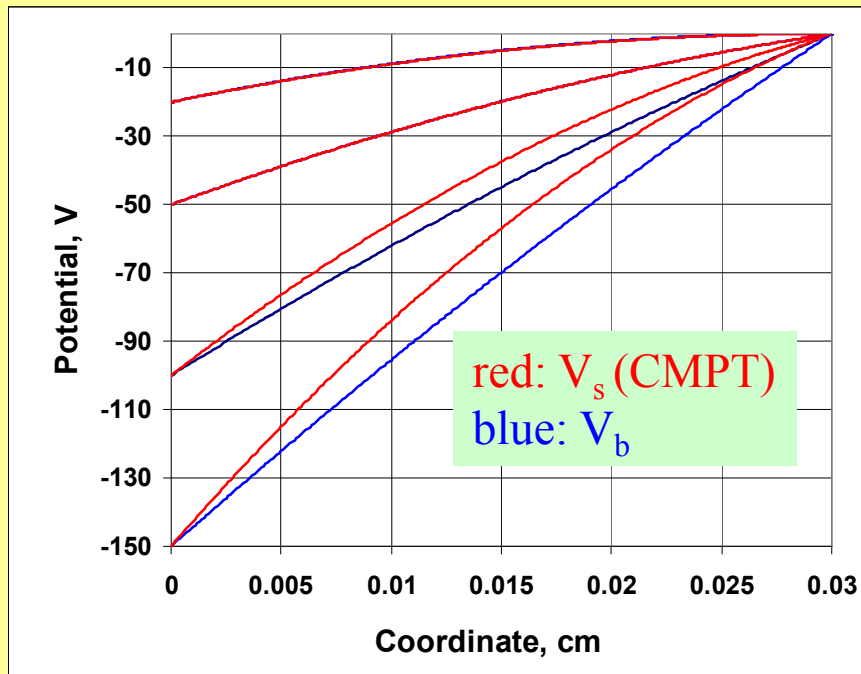
Main features:

- ✓ Potential is nonlinear
- ✓ $E(x)$ is not constant
- ✓ Slope of $E(x)$ grows with voltage

disagreement with resistive edge model

Potential and E_z distributions based on CMPT data

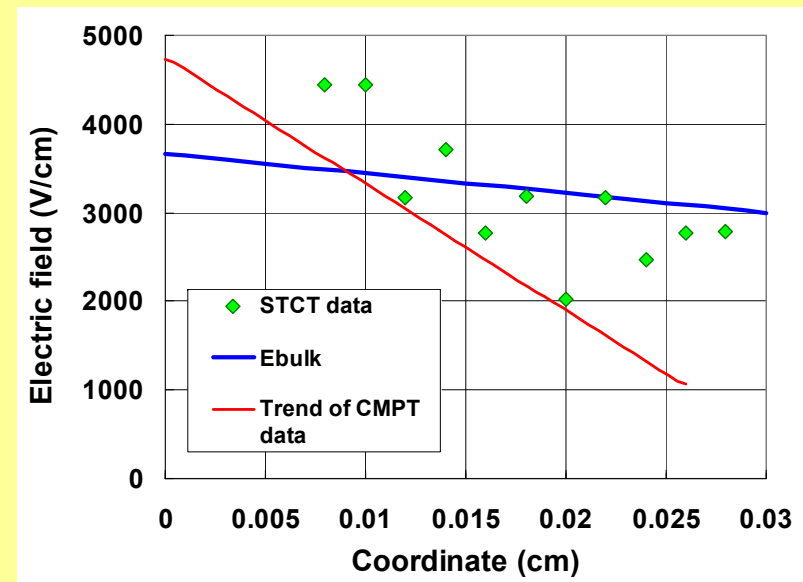
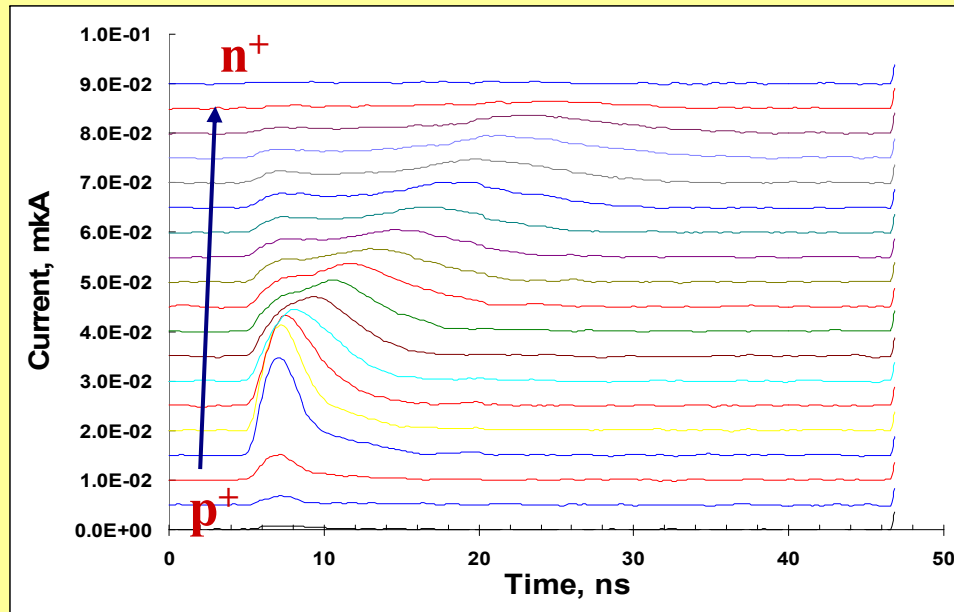
E_z sign inversion



Experimental results on surface potential are in agreement to the amorphous edge model

E_{xs} derived from STCT

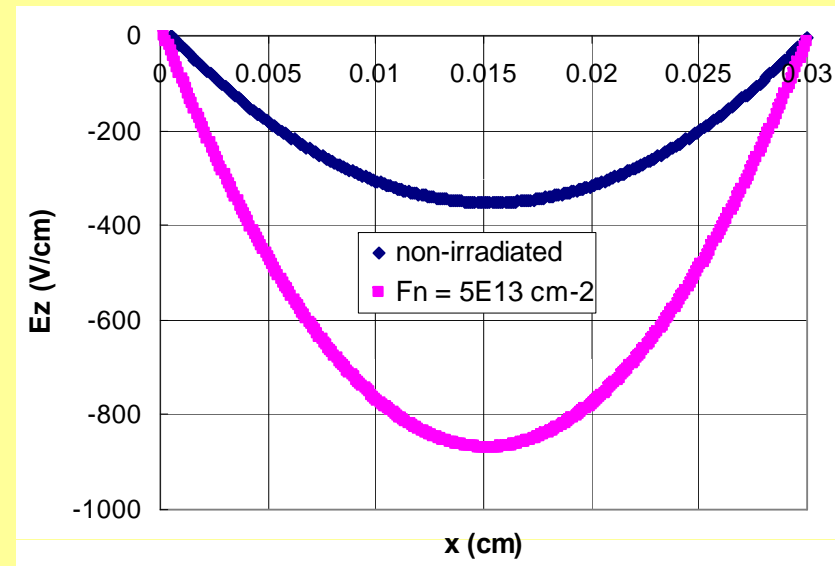
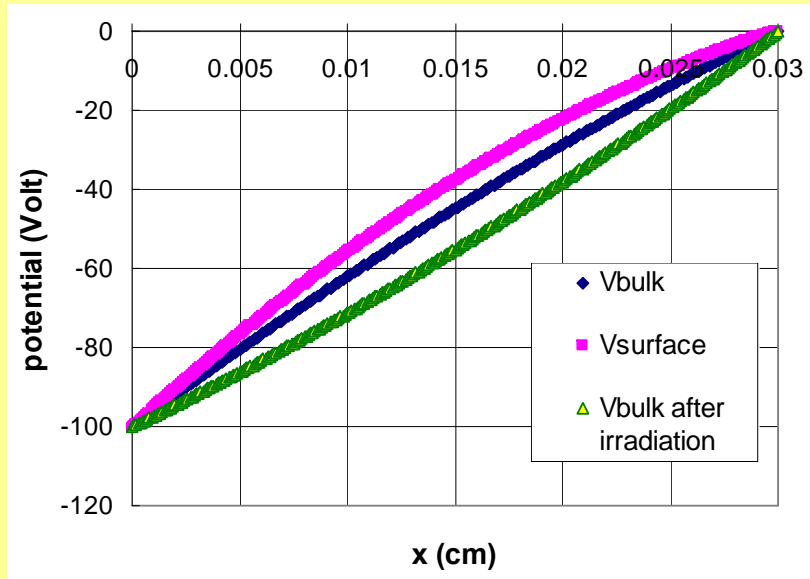
$V = 100 \text{ V}$, $V_{fd} = 20 \text{ V}$, $d = 300 \text{ }\mu\text{m}$



$$\text{At } V > V_{fd} \quad E(x) = \frac{2V_{fd}}{d} \left(1 - \frac{x}{d}\right) + \frac{V - V_{fd}}{d}$$

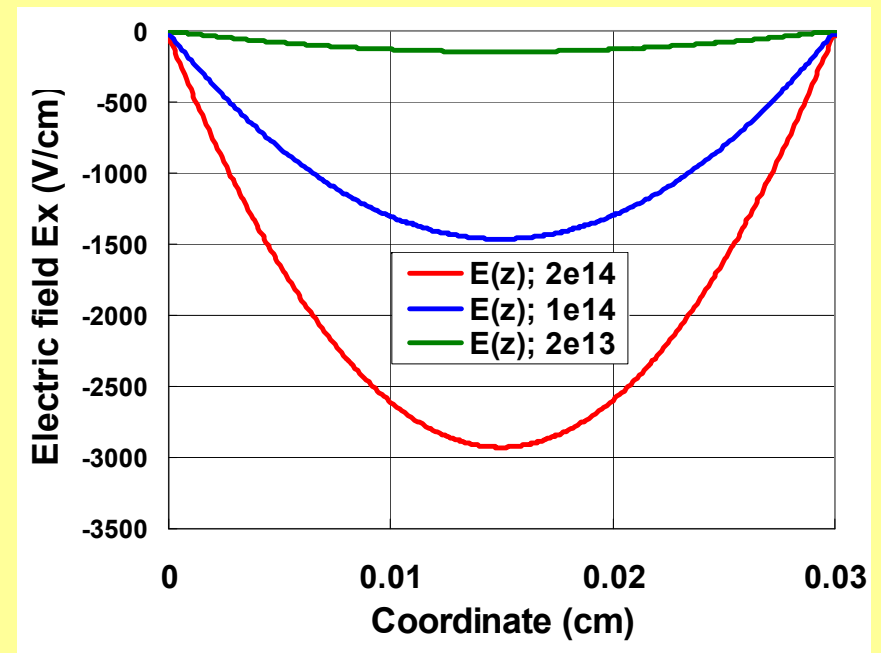
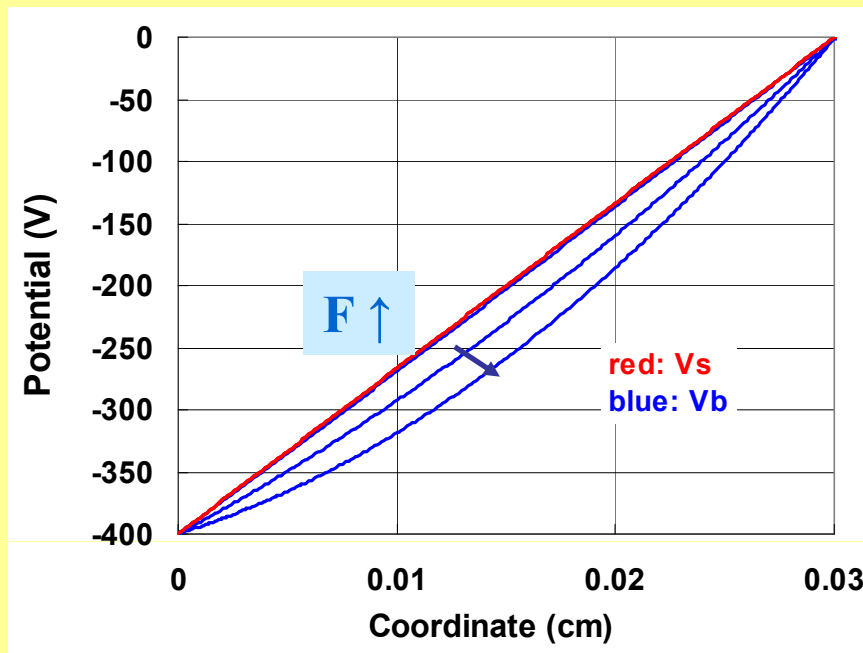
Results on $E_x(x)$ derived from CMPT and STCT show the same tendency of E_s reduction

E_z simulation in irradiated p -on- n edgeless detectors



E_z simulation in irradiated p -on- n detectors

$V = 400$ V



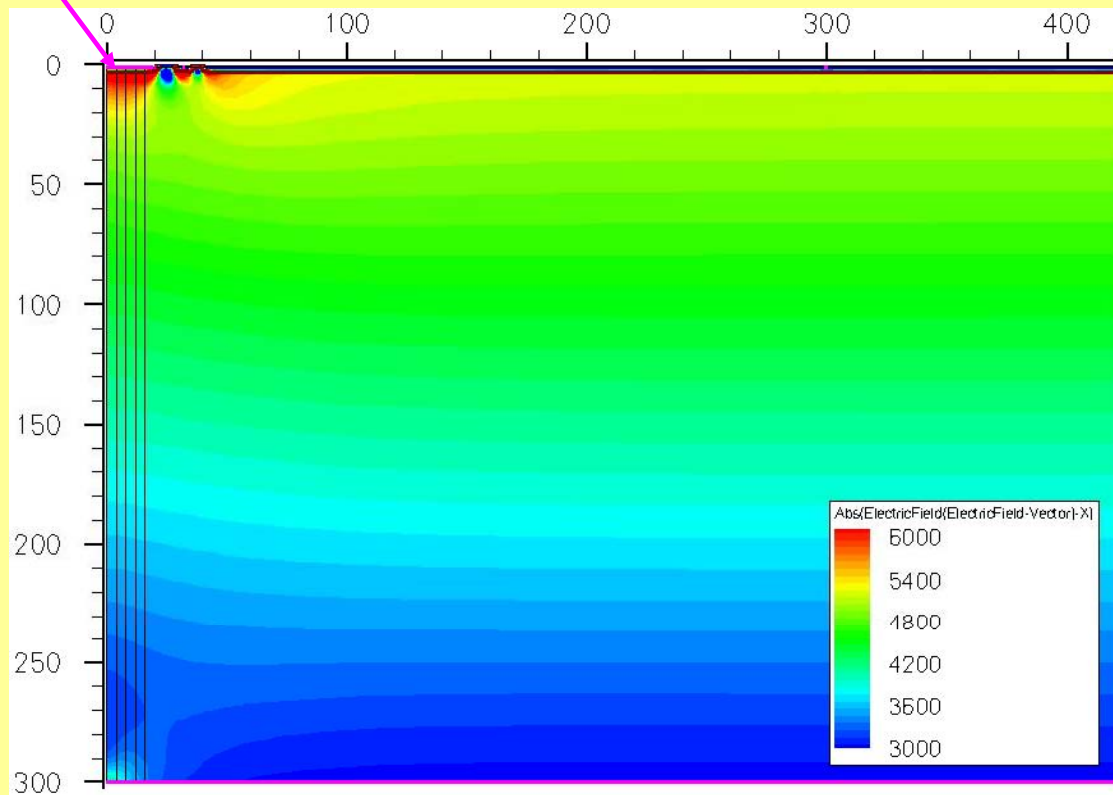
E_z is \sim kV/cm and increases with fluence \rightarrow
predicts the increase of the hole current flow into the bulk
and corresponding increase of the bulk current.

$E(x)$ simulation using ISE-TCAD

J.P. Balbuena et al., CNM, Barcelona, presented at NSS-2008 **and are in progress**

CTR

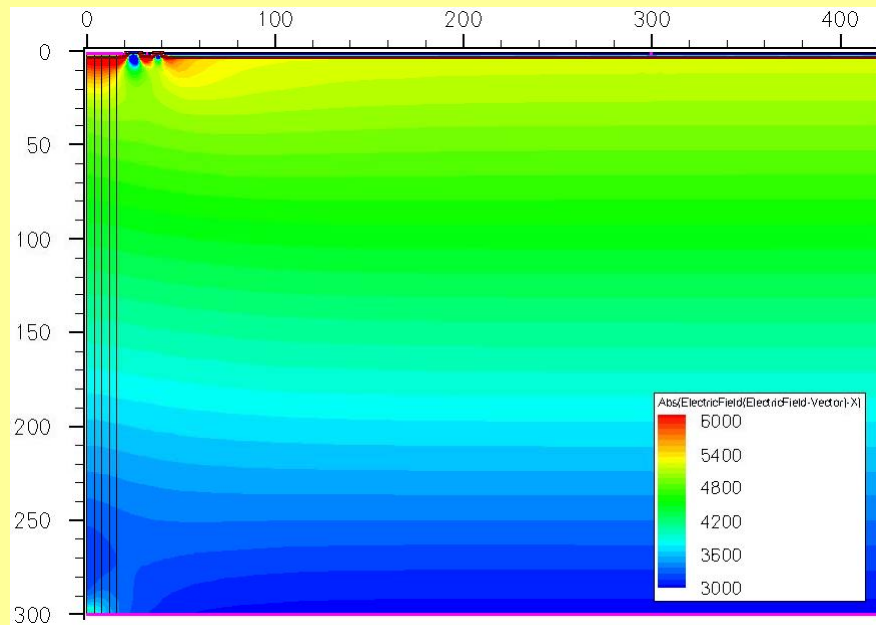
p-on-n detector, saw cut edge



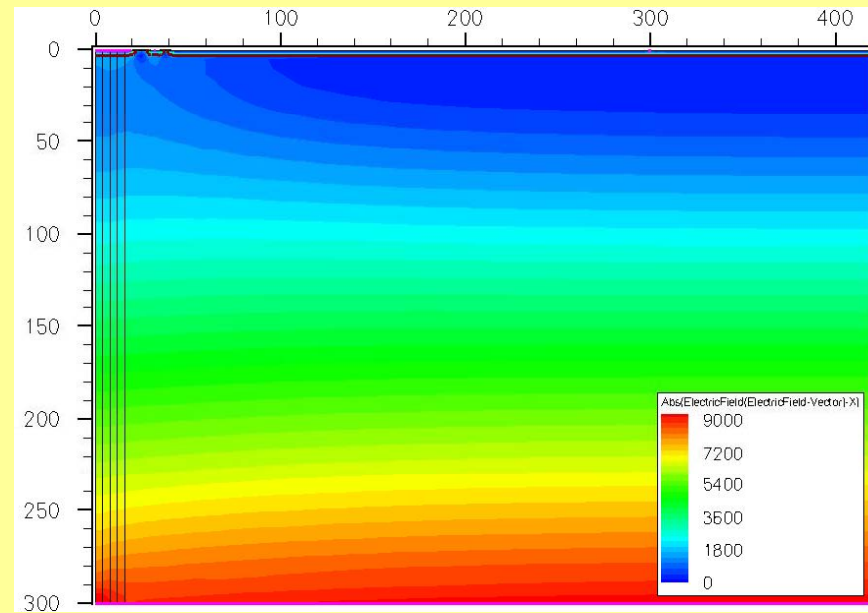
Electric field at the front contact is maximal at CTR (10 to 50 μm from the edge) and becomes lower under the strips

E_z simulation in irradiated *p-on-n* detectors (preliminary)

Non-irradiated

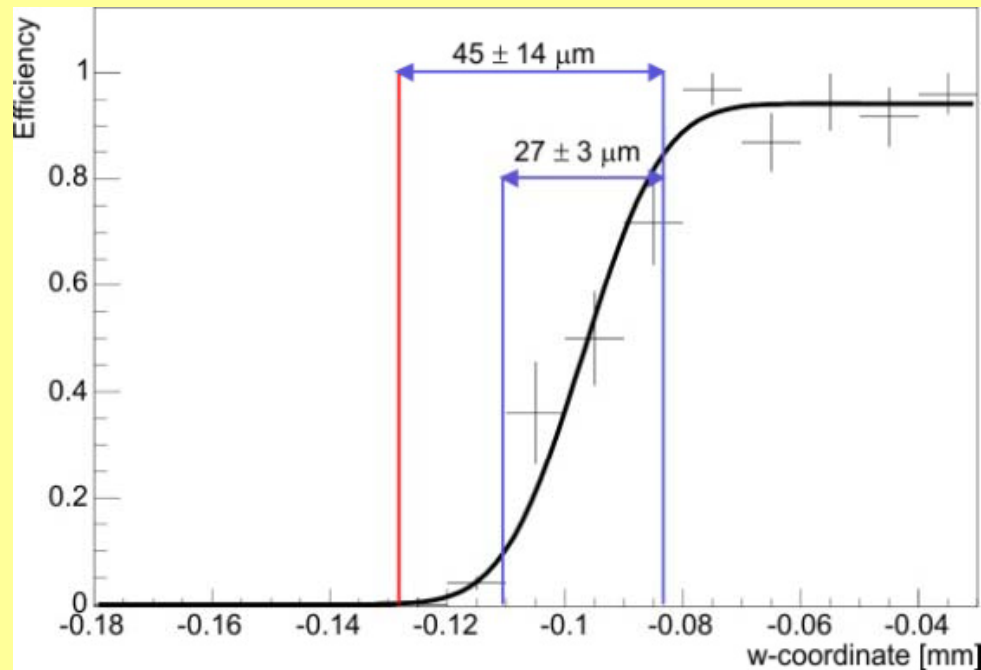


$F_n = 4 \cdot 10^{14} \text{ cm}^{-2}$



Recent experimental results on CCE in p-on-n edgeless detectors with CTS

Efficiency of CTS detector at the sensitive edge

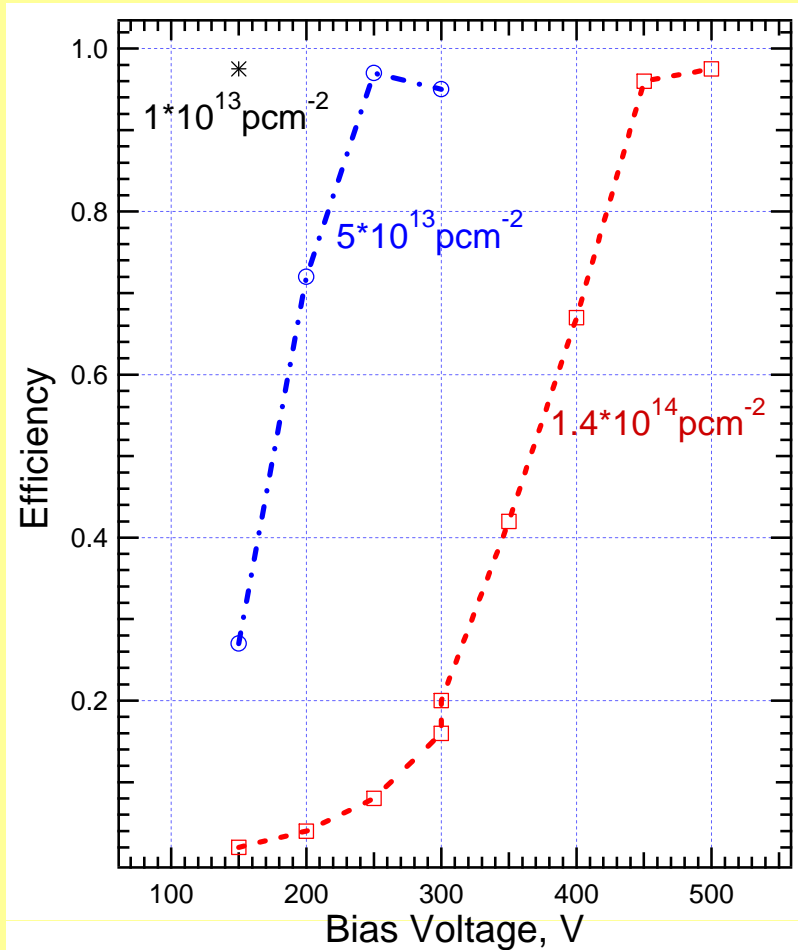


The left-most vertical line indicates the reconstructed position of the physical edge, the other two vertical lines indicate the 10%-90% efficiency rise interval.

Diminished non-sensitive width of 47 μm is achieved!

G. Ruggiero et al. Planar Edgeless Silicon Detectors for the TOTEM Experiment.
Pres. 8th Intern.Conf. on Position Sensitive Detectors (PSD8), Glasgow, Sept 1-5, 2008,
Nucl. Instr. and Meth. A (in press).

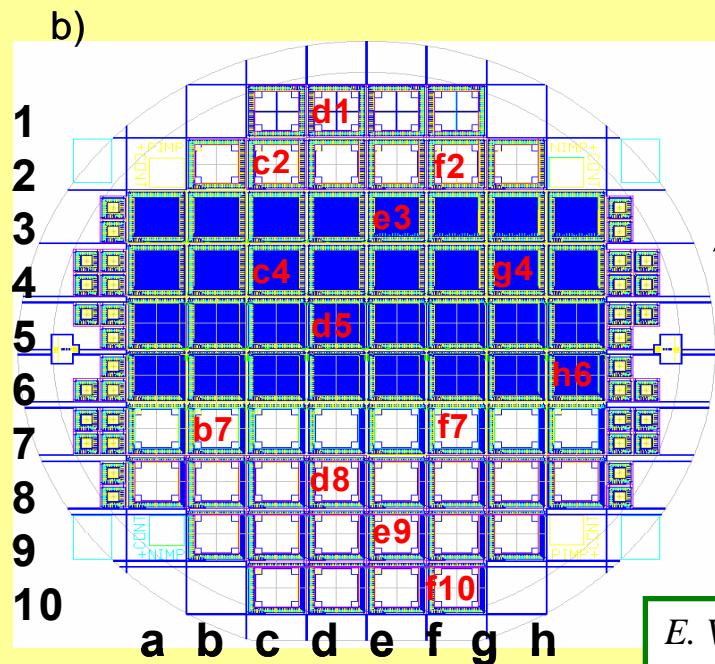
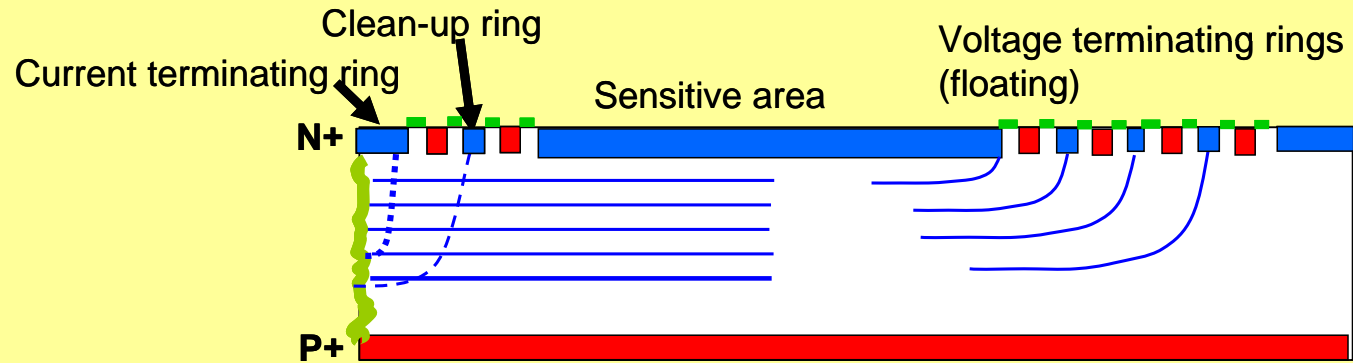
CCE in irradiated p-on-n edgeless detectors with CTS



24 GeV/c protons
T = -18C

The efficiency has been calculated by comparing the hits in the irradiated detector with the hits in a non-irradiated detector placed in front, along the beam axis.

Development of *n-on-p* edgeless detectors with CTS



Layout: 10 different designs

MCZ p-type Si

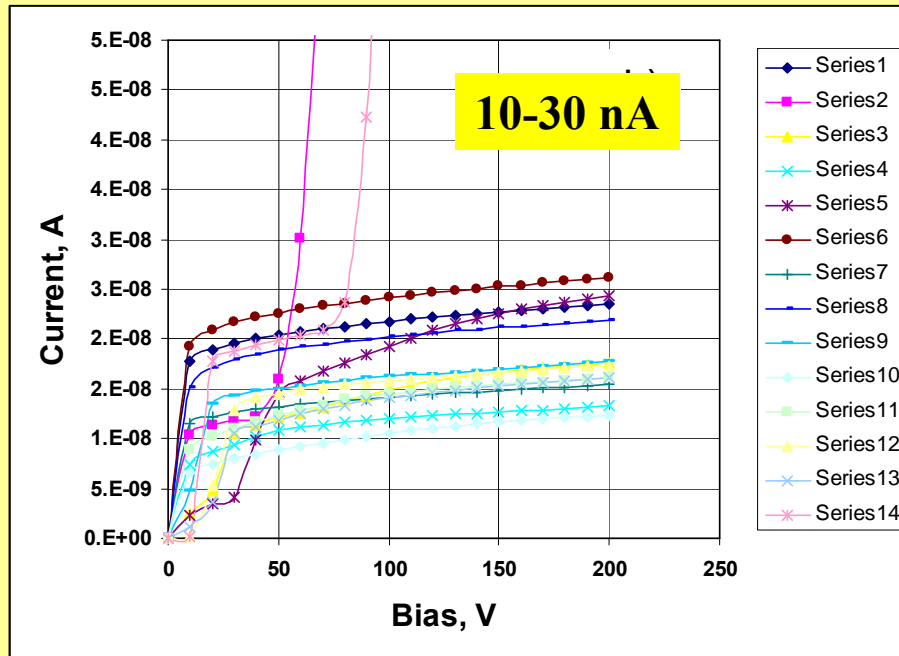
Processed by Ioffe&RIMST

E. Verbitskaya et al., 13 RD50 Workshop, CERN, Nov 10-12, 2008

I-V characteristics of n-on-p edgeless detectors

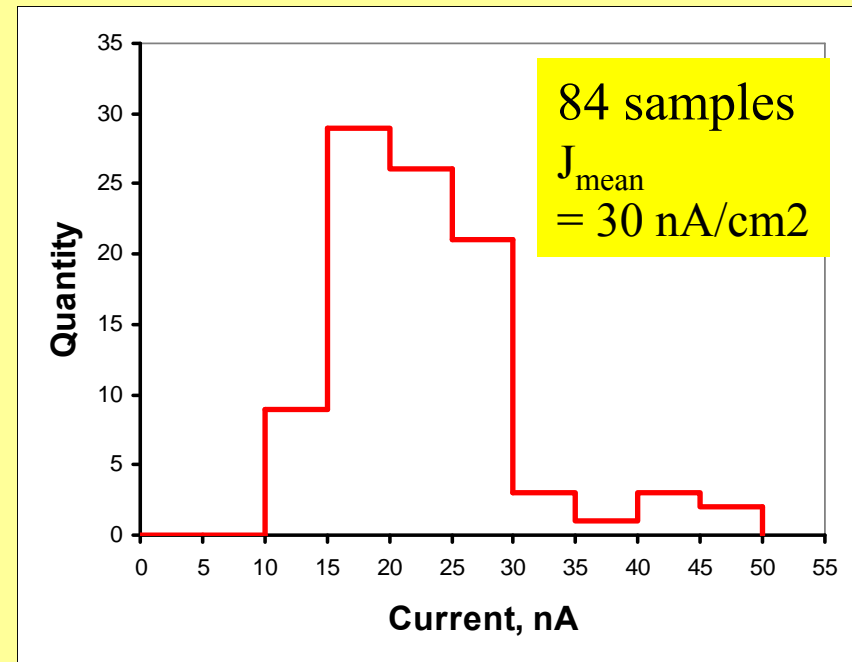
I-V characteristics

14 randomly selected detectors
with different design



Statistics of reverse current

$V = 200 \text{ V}$; $S = 8 \times 8 \text{ mm}^2$



MPT and TCT measurements are in progress!

Conclusions

- ✔ **Performance of edgeless detectors with CTS allows realization of edgeless detectors which characteristics are controlled by the bulk properties**
- ✔ **The model of amorphous edge is adequate to the experimental results on n-on-p edgeless detectors**
- ✔ **In detectors with CTS diminished non-sensitive width of 47 μm is achieved**
- ✔ **N-on-P edgeless strip detector seems to be radiation hard that needs experimental testing**

Acknowledgements

This work was done in the frame of INTAS-CERN project # 03-52-5744

and supported in part by:

- RF President Grant # 2951.2008.2,
- contract of Russian Agency on Science and Innovation # 2.516.11.6098

Thank you for your attention!